Optical properties of the quasi-two-dimensional dichalcogenides 2H-TaSe$_2$ and 2H-NbSe$_2$

S.V. Dordevic[1], D.N. Basov[1], R.C. Dynes[1], B. Ruzicka[2], V. Vescoli[2], L. Degiorgi[2,a], H. Berger[3], R. Gaál[3], L. Forró[3], and E. Bucher[4]

[1] Department of Physics, University of California, San Diego, La Jolla CA 92093, USA
[2] Laboratorium für Festkörperphysik, ETH Zürich, 8093 Zürich, Switzerland
[3] Institute of Physics of Complex Matter, EPF Lausanne, 1015 Lausanne, Switzerland
[4] Lucent Technologies, Murray Hill, NJ 07974, USA and Fakultät für Physik, Universität Konstanz, 78457 Konstanz, Germany

Abstract. We present a comprehensive analysis of the optical constants of the two-dimensional dichalcogenide materials 2H-TaSe$_2$ and 2H-NbSe$_2$, in an attempt to address the physics of two-dimensional correlated systems. The title compounds were studied over several decades in frequency, from the far-infrared to the ultraviolet. Measurements with linearly polarized light have allowed us to obtain both the in-plane and out-of-plane components of the conductivity tensor. Although the electromagnetic response of dichalcogenides is strongly anisotropic, both the in-plane and out-of-plane components of the conductivity tensor share many common features, including the presence of a well-defined metallic component, as well as a "mid-infrared band". We discuss the implications of these results in the context of the spectroscopic results of other classes of low-dimensional conductors such as the high-temperature superconducting cuprates. In particular, the analysis of the redistribution of the spectral weight as a function of temperature, as well as the behavior of the quasiparticles relaxation rate, points to significant distinctions between the charge dynamics of dichalcogenides and other classes of low dimensional conductors.

PACS. 78.20.-e Optical properties of bulk materials and thin films – 71.45.Lr Charge-density-wave systems – 74.25.Gz Optical properties

1 Introduction

Electronic and magnetic properties of two dimensional (2D) electron gas have been at the focus of condensed matter physics for many decades [1]. An interesting aspect of these systems is the competition and/or coexistence between different electronic ground states. Several classes of dichalcogenides are well suited for the examination of 2D electron gas in the frequency domain. Indeed, large single crystals of various dichalcogenides permit investigation of carrier dynamics using infrared and optical spectroscopy. The layered crystal structure predestines strong anisotropy between in-plane (*ab*) and inter-plane (*c*-axis) response. In these systems the 2D electron gas reveals charge-density-wave (CDW) instabilities occurring at temperatures above the critical temperature T_c of the superconducting transition. This particular feature of dichalcogenides is especially intriguing in view of the anomalous properties of another class of strongly anisotropic layered materials such as the high-T_c cuprate superconductors (HTC). Complexity of electronic and magnetic properties of HTC is commonly attributed

to a delicate balance of competing interactions producing superconducting pairing, spin, charge and orbital ordering [2]. On the contrary, magnetic and orbital degrees of freedom are unlikely to play an important role in dichalcogenides. Therefore, the latter class of materials allows one to isolate the effects associated with density wave instabilities and to explore the role of these effects for the dynamics of the correlated quasi-2D electron gas. Two members of the dichalcogenides family, 2H-TaSe$_2$ and 2H-NbSe$_2$, are particularly relevant in this respect. The former compound reveals two CDW phase transitions: an incommensurate triple one at $T_{1\text{CDW}} = 122$ K and a first-order lock-in transition to a commensurate phase at $T_{2\text{CDW}} = 90$ K (Ref. [3]). 2H-NbSe$_2$ undergoes a second-order phase transition to an incommensurate CDW state at $T_{\text{CDW}} = 33$ K which coexists with superconductivity below $T_c = 7.2$ K (Ref. [4]). The pronounced quasi-2D nature of the crystallographic structure of these two compounds leads to approximately cylindrical Fermi surfaces. In contrast with the 1D case, however, 2D dichalcogenide materials remain metallic in the presence of CDW since the Fermi surface-driven instabilities are generally weaker than in 1D systems. In these 2D systems energy gaps can open only at

ᵃ e-mail: degiorgi@solid.phys.ethz.ch

discrete fragments of the Fermi surface, where nesting occurs. The quasi-2D systems also do not present peculiar 1D spectroscopic properties, for which a possible Luttinger liquid scenario has been suggested [5].

Infrared (IR) and optical spectroscopy have emerged as powerful techniques for the examination of correlation effects and electron dynamics in a large variety of materials [6–8]. Optical methods are especially informative for probing anisotropy of the electronic transport in layered compounds. Measurements with polarized light deliver important information on both the in-plane and inter-plane response of quasi-2D solids. Here, we particularly focus our attention on the anisotropy of the normal state electrodynamics with the goal to report the complete analysis of the optical response of 2H-TaSe$_2$ and 2H-NbSe$_2$; we will not address the optical response of 2H-NbSe$_2$ in the superconducting state. The main bulk of our experimental data has been already published [9–11]. In our previous publications, however, the analysis of the spectral weight distribution on 2H-NbSe$_2$ as well as a thorough discussion of the frequency dependence of the scattering rate in 2H-TaSe$_2$ were not presented. Therefore, we will emphasize here common as well as contrasting features of these two compounds in a unified and comprehensive presentation. The analysis of the electronic spectral weight and its distribution at low T, as well as the temperature and frequency dependence of the quasiparticle scattering rate extracted from IR measurements, will be the main goal of this work and will be used to shed light on the nature of collective states in highly anisotropic systems without CuO$_2$ units in their structure. The pertinent comparison with HTC compounds, for instance with respect to the issue of coherent versus incoherent anisotropic response, will be developed throughout the discussion.

2 Sample characterization and experimental technique

High quality single crystals (2H-TaSe$_2$ grown at EPFL and 2H-NbSe$_2$ grown at Lucent) were prepared from the elements by a reversible chemical reaction with iodine as a transport agent [12]. The sample growth conditions for 2H-TaSe$_2$ were optimized for making thick single crystals. The sample 2H-TaSe$_2$ used in the optical study had ab-plane dimensions of 5×5 mm^2, while in the c-axis direction it was 4 mm long. Typical dimensions of 2H-NbSe$_2$ single crystals employed for the optical measurements were $4 \times 4 \times 1$ mm^3.

The dc transport measurements were performed with a conventional four-probe technique and thoroughly reported in references [9–11]. Here, we just recall the main features. The temperature dependence of the resistivity of 2H-TaSe$_2$ along the c-axis $\rho_c(T)$ is qualitatively similar to the one probed within the ab-plane $\rho_{ab}(T)$ despite the fact that the absolute values are strongly anisotropic. The anisotropy ratio ρ_c/ρ_{ab} is as high as 25 at 300 K and increases up to 50 as temperature is lowered down to about 100 K. Above the CDW phase transition at

122 K, the c-axis resistivity $\rho_c(T)$ is increasing monotonically, with a tendency to saturation around 400 K. The in-plane resistivity reveals nearly linear behavior between 120 and 400 K. The temperature dependence of $\rho_{ab}(T)$ for 2H-NbSe$_2$ displays the superconducting phase transition and a weak and barely observable anomaly at the CDW critical temperature. Similar to 2H-TaSe$_2$ the in-plane resistivity $\rho_{ab}(T)$ of 2H-NbSe$_2$ is again monotonic and approximately linear in T. It was not possible to measure $\rho_c(T)$ on our 2H-NbSe$_2$ microcrystals. However, previously published data on the c-axis resistivity $\rho_c(T)$ of 2H-NbSe$_2$ revealed metallic and almost linear temperature dependence between room temperature and T_c (Ref. [13]). The anisotropy ratio $\rho_c(T)/\rho_{ab}(T)$ is found to be around 30 between room temperature and 100 K, and to decrease to about 10 at 10 K.

Reflectivity measurements $R(\omega)$ of 2H-TaSe$_2$ have been performed over a frequency range from 20 to 10^5 cm^{-1} on mechanically polished samples [9,10]. The polishing procedure produced an optically flat surface and did not lead to an unwanted "contamination" of the c-axis data with the features of the in-plane response. IR and visible reflectivity of small 2H-NbSe$_2$ single crystals was measured with a set-up specially adapted for spectroscopy of micro-crystals [11]. In this case as-grown surfaces were used in order to rule out extrinsic effects due to polishing. Optical data on large single crystals of 2H-NbSe$_2$ grown at EPFL, with polished surfaces, produced equivalent results. The real part $\sigma_1(\omega)$ of the optical conductivity was obtained by Kramers-Kronig (KK) transformation of the $R(\omega)$ spectra, appropriately extended with standard extrapolations [14] at low and high frequencies [9–11]. In the region between 2.5 and 4 eV, the in-plane reflectivity measurements of 2H-NbSe$_2$ were also supplemented with spectroscopic ellipsometry. Ellipsometric measurements directly yield both the real and imaginary parts of the optical constants, without the need for KK analysis. However, excellent agreement has been established in the overlapping region of the two methods, indicating that KK analysis is reliable [9–11].

3 Results and analysis

In Figure 1, we plot on a log-log scale the optical conductivity determined from the KK analysis of the reflectivity data. We have merged in this figure the original spectra, previously published in references [9–11], as comprehensive summary of the data and as starting point for the present discussion. Here, we only show the data up to 1 eV in order to emphasize the temperature dependence of $\sigma_1(\omega)$. Additionally on the y-axis of Figure 1, we have indicated the measured dc values of the conductivity at different temperatures [9–11]. There is a fair agreement with the dc-limit (i.e., $\omega \rightarrow 0$) of $\sigma_1(\omega)$, suggesting that the Hagen-Rubens (HR) extrapolation [14], used for the KK transformation, is consistent with the dc transport results. We also stress that neither the topics nor the conclusions of our work are affected by the HR extrapolation
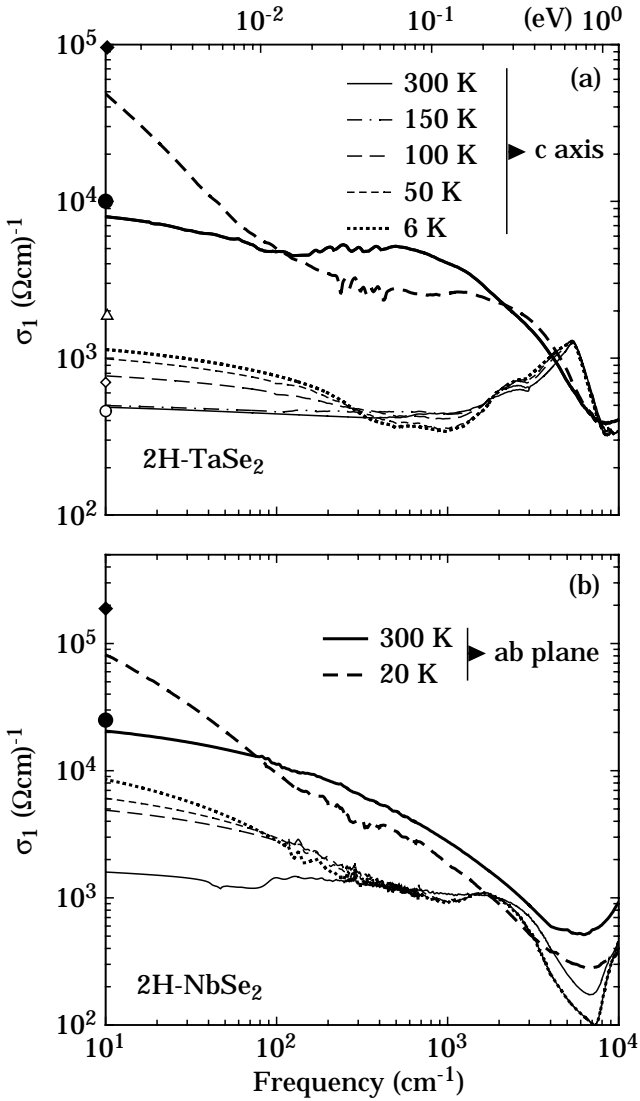
Fig. 1. Temperature dependence of the real part $\sigma_1(\omega)$ of the optical conductivity for (a) 2H-TaSe$_2$ and (b) 2H-NbSe$_2$ within the *ab*-plane and along the *c*-axis [9–11]. The legends apply for both panels. (Note the double logarithmic axes.) The symbols indicate the σ_{dc} values, extracted from the resistivity [9–11]: for 300 and 20 K in the *ab*-plane and for 300, 100 and 6 K along the *c*-axis, respectively. Below 20 cm^{-1}, the spectra of the optical conductivity are the consequence of the Hagen-Rubens extrapolation of the measured reflectivity (see text).

and by the shape of $\sigma_1(\omega)$ at low energies. A quick inspection of Figure 1 shows that the conductivity is metallic for both in-plane and inter-plane directions. The dominant feature of the FIR conductivity for both polarization directions is the zero-energy (metallic) peak that narrows with decreasing temperature. This narrowing is particularly strong in the *c*-axis response where the metallic feature in the low temperature $\sigma_1(\omega)$ data emerges out of flat conductivity at 300 K. Generally, the narrowing of the zero-energy (metallic) resonance is signaling the suppression of quasiparticles scattering and may also result from

the redistribution of the electronic spectral weight [14]:

$$N(\omega) = \int_0^\omega \sigma_1(\omega')\mathrm{d}\omega' \tag{1}$$

in the conductivity. This latter possibility will be discussed below.

In addition to the zero-energy resonance we observe several other absorption bands in the optical response of both dichalcogenides. The *c*-axis conductivity of both systems reveals a broad mid-infrared (MIR) structure centered at 6000 cm^{-1} for 2H-TaSe$_2$ (Fig. 1a) and 2000 cm^{-1} for 2H-NbSe$_2$ (Fig. 1b). The *c*-axis spectra of 2H-TaSe$_2$ display an additional feature at about 2000 cm^{-1} (Fig. 1a). All these peaks are most prominent at low temperatures but can be identified even in the 300 K data, which rules out their direct connection to the CDW transitions. Furthermore, both materials show a depression of the inter-plane conductivity with a "notch" feature at about 1000 cm^{-1}. This latter feature also develops gradually with decreasing T and again is therefore unlikely to be directly related to the onset of the CDW state. In particular, one can clearly identify the notch structure in the data for 2H-TaSe$_2$ at temperatures well above the CDW transition.

The real part of the *ab*-plane conductivity of 2H-TaSe$_2$ (Fig. 1a) is also characterized at all temperatures by a broad MIR absorption overlapping with the low frequency metallic contribution. Below room temperature there is a redistribution of spectral weight between the two components accompanied by a progressive narrowing of the zero-energy resonance in the FIR range, as already noted above. The broad maximum of the MIR absorption shifts slightly towards higher frequency (*i.e.*, from approximately 0.07 eV up to 0.08 eV) between 300 and 80 K and in a more pronounced way (to about 0.15 eV at 10 K) below 80 K [9]. The onset of the commensurate phase transition at T_{2CDW} leaves the excitation spectrum, as well as transport and thermodynamic [3] properties almost unaffected. The optical response of 2H-NbSe$_2$ within the *ab*-plane (Fig. 1b) bears some similarities with that of 2H-TaSe$_2$. Besides the pronounced narrowing of the metallic component with decreasing temperature, no new features can be observed at $T < T_{CDW}$. It appears that the CDW transition has a somewhat stronger impact on the electronic properties of 2H-TaSe$_2$ than of 2H-NbSe$_2$. It is interesting to remark the strong analogies of the optical spectra of these dichalcogenides with the excitation spectra of other two dimensional systems, like HTC [15] and the organics (BEDT-TTF)$_2$[Cu(SCN)$_2$] (Ref. [16]) and (BEDT-TTF)$_4$(Ni(dto)$_2$] (Ref. [17]). The zero-energy (metallic) mode and its narrowing with decreasing temperature as well as the MIR absorption seem to be generic features of 2D layered-like correlated systems.

Further insight into the charge dynamics can be achieved by exploring changes of the electronic spectral weight $N(\omega)$ defined in equation (1). $N(\omega)$ is proportional to the number of charge carriers participating in the optical absorption below a cut-off frequency ω. The results of the spectral weight analysis using equation (1) are shown
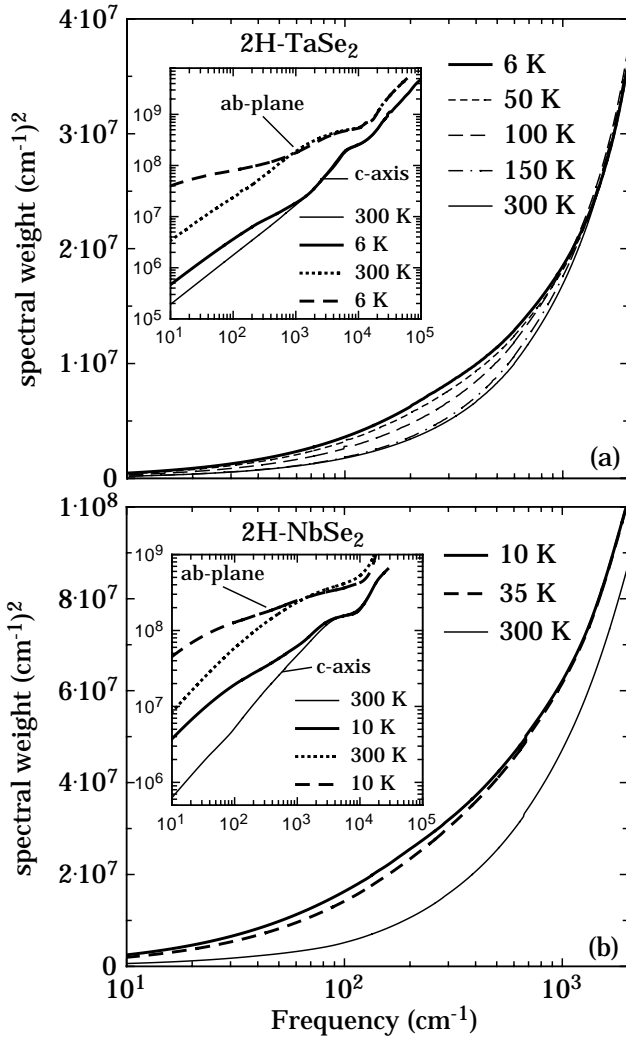
Fig. 2. Temperature dependence of the integrated spectral weight (Eq. (1)) for (a) 2H-TaSe$_2$ (Ref. [10]) and (b) 2H-NbSe$_2$ along the c-axis in the mid-infrared spectral range. The insets show the same quantity up to 10^5 cm^{-1} for both polarizations.

in Figure 2. The spectral weight analysis was originally done for the c-axis response of 2H-TaSe$_2$ only [10], which will be displayed here again for comparison purpose. The main panels of Figure 2 display the temperature dependence of the spectral weight distribution along the c-axis in the far- and mid-IR, whereas the insets give an overview of the spectral weight evolution up to 10^5 cm^{-1} for both polarizations. The spectral weight progressively shifts to the low frequency range as temperature is lowered from 300 K to 10–20 K in either the in-plane or inter-plane response of both dichalcogenides studied here. Specifically, the spectral weight from the notch feature in the c-axis conductivity is translated to low energies and predominantly accounts for the increase of $\sigma_1(\omega)$ in FIR.

Although the optical conductivity is metallic for both polarizations (Fig. 1), a more detailed examination of $\sigma_1(\omega)$ suggests that its frequency dependence differs from the Lorentzian form prescribed by the Drude theory. Experimentally these deviations are best identified within

the so-called "extended" Drude formalism [15]. In this approach one inverts the Drude formula of the complex optical conductivity $\sigma(\omega)$ to determine the frequency dependence of the scattering rate:

$$\Gamma(\omega) = \frac{1}{\tau(\omega)} = \frac{\omega_p^2}{4\pi} \text{Re}\left(\frac{1}{\sigma(\omega)}\right). \tag{2}$$

In equation (2) the squared plasma frequency $\omega_p^2 = \frac{4\pi n e^2}{m^*}$ (n is the carrier density and m^* their effective mass) can be obtained from the integration of the real part of the optical conductivity $\sigma_1(\omega)$ up to the cut-off frequency W in equation (1), which usually corresponds to the onset of inter-band absorptions. In this fashion, ω_p considered here is the total spectral weight encountered in the optical conductivity within the spectral range of the intra-band excitation (*i.e.*, the band width is of the order of $2W$). In order to fully account for the intraband excitations, we choose the cut-off frequency $W = 8000$ cm^{-1} for the ab-plane and $W = 2000$ cm^{-1} for the c-axis for both compounds. These values of W lead to $\omega_p^{ab} = 22\,816$ and $20\,200$ cm^{-1}, and $\omega_p^c = 6017$ and $13\,000$ cm^{-1} for 2H-TaSe$_2$ and 2H-NbSe$_2$ (Fig. 2), respectively.

The frequency dependence of the scattering rate was already presented in reference [11] for 2H-NbSe$_2$. In order to allow a comparison with the corresponding analysis for 2H-TaSe$_2$, shown here for the first time, we display $\Gamma_c(\omega)$ and $\Gamma_{ab}(\omega)$ in parallel for both compounds. Figure 3 shows the results of the scattering rate analysis (Eq. (2)) for the out-of-plane direction, whereas Figure 4 displays similar analysis of the in-plane data. The c-axis scattering rate of 2H-NbSe$_2$ (Fig. 3b) looks slightly different from the one originally reported in reference [11], since here no subtraction of finite energy excitations was performed. Indeed, for the calculations of $\Gamma(\omega)$ along both polarization directions one can subtract finite energy excitations (like, *e.g.*, the one at about 2000 cm^{-1} in 2H-NbSe$_2$ along the c-axis [11]) from the experimental optical conductivity, in order to single out the effective intra-band contribution. This latter approach requires specific choices and some *ad hoc* interpretations of the data. However regardless of the method employed, the general trends of $1/\tau(\omega)$ spectra are preserved and changes occur primarily at higher frequencies where the use of equation (2) is questionable in the first place.

At low temperature we observe a characteristic suppression of $1/\tau_c(\omega)$ below 500 and 1000 cm^{-1} for 2H-TaSe$_2$ and 2H-NbSe$_2$, respectively. In contrast with the ab-plane data, the spectra of the c-axis scattering rate for both compounds reveals saturation at frequencies above 1500 cm^{-1} (Fig. 3). This trend is consistent with the dominant role of electron-phonon interaction in the scattering processes [15]. The lack of saturation in the $1/\tau_{ab}(\omega)$ data (Fig. 4) is indicative of inelastic scattering channels with characteristic energies beyond that of the lattice modes and could be directly caused by the mid infrared absorption band. One also notices several important differences in the behavior of the $1/\tau_{ab}(\omega)$ spectra of 2H-TaSe$_2$ and 2H-NbSe$_2$. In the latter compound the temperature dependence of the in-plane scattering rate is restricted to
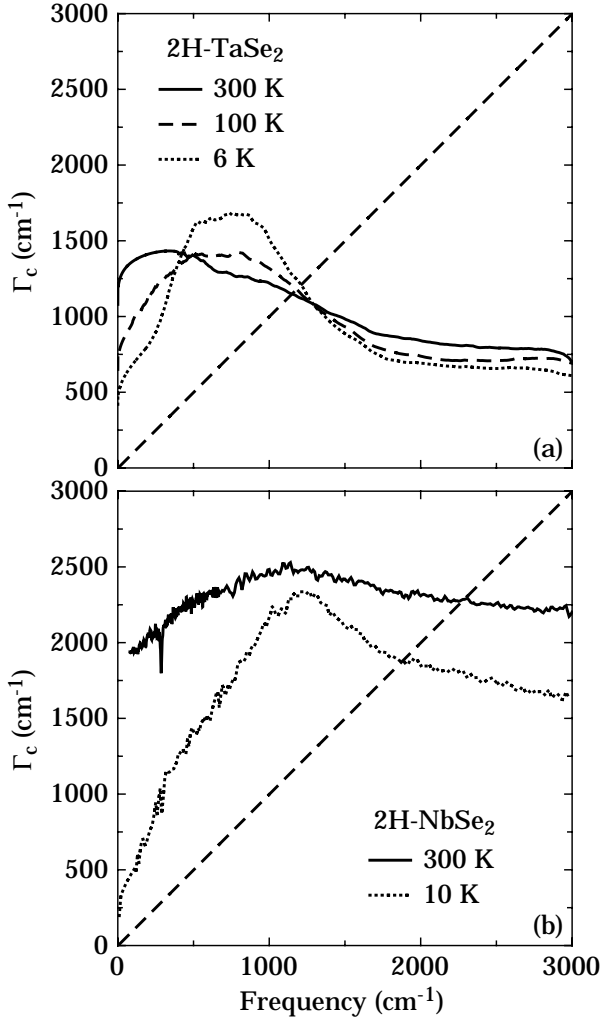
Fig. 3. Temperature dependence of the scattering rate after equation (2) for (a) 2H-TaSe$_2$ and (b) 2H-NbSe$_2$ (Ref. [11]) along the *c*-axis in the mid-infrared spectral range. The dashed line indicates the situation where $1/\tau(\omega) \sim \omega$.

Fig. 4. Temperature dependence of the scattering rate after equation (2) for (a) 2H-TaSe$_2$ and (b) 2H-NbSe$_2$ (Ref. [11]) within the *ab*-plane in the mid-infrared spectral range. The dashed line indicates the situation where $1/\tau(\omega) \sim \omega$.

nearly parallel shifts of the spectra, whereas 2H-TaSe$_2$ reveals significant changes in the frequency dependence of $1/\tau_{ab}(\omega)$. Suppression of the scattering rate at lower energies clearly seen in the 20 K data is followed by an overshoot with respect to the spectra taken at 100 K and at 300 K. This functional form of the $1/\tau_{ab}(\omega, 20\ \mathrm{K})$ data might be suggestive of the formation of a partial gap in the electronic density of states [18]. These features and the possible role of the CDW state in the observed trends will be further discussed in the following section.

4 Discussion

4.1 Charge density wave transition and infrared response of dichalcogenides

Our optical results for both compounds do not display any clear cut signatures of a CDW gap within the *ab*-plane,
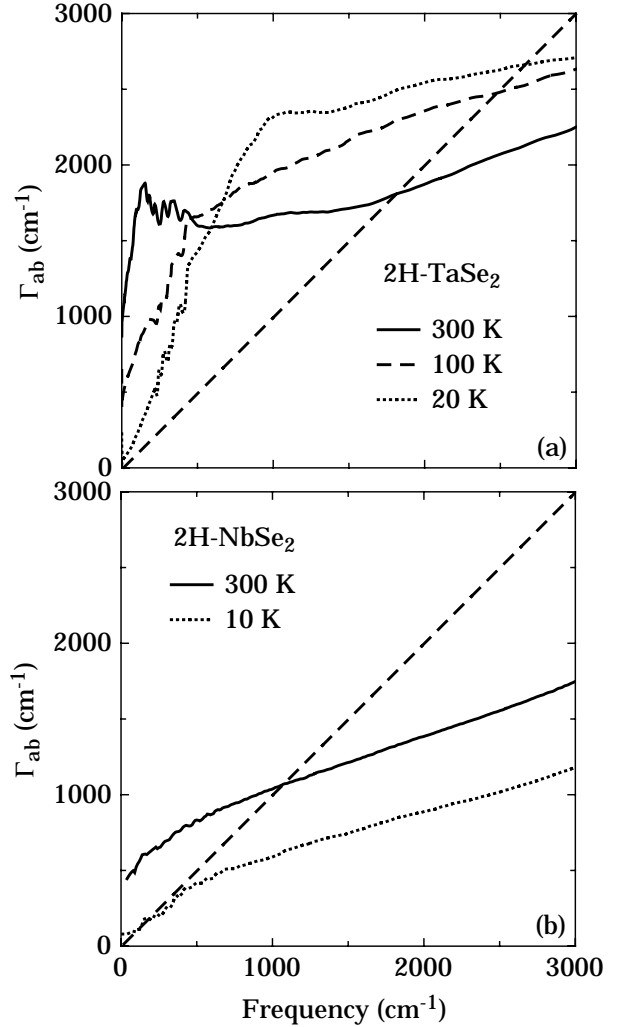
developing below the onset of CDW phase transitions, which is not unexpected from the two-dimensionality of these materials [19]. Nevertheless, within a CDW scenario one might expect the appearance of some precursor effects [19–22]. Therefore, fluctuations associated with short range CDW segments can be expected to occur in 2D dichalcogenide systems, as well. We have previously conjectured that those fluctuation effects in 2H-TaSe$_2$ might lead to a suppression of $\sigma_1(\omega)$ within the *ab*-plane at about 0.07 eV (*i.e.*, the MIR absorption) already below 300 K (Ref. [9]). One could associate such a suppression of $\sigma_1(\omega)$ with the optical manifestation of the CDW pseudogap (*i.e.*, a gap that opens only over limited parts of the Fermi surface). A crossover to a long range ordered CDW state below $T_{1\mathrm{CDW}}$ in 2H-TaSe$_2$ and its lock-in state at $T_{2\mathrm{CDW}}$ further suppress the scattering channels, causing the sharp drop in the resistivity [9–11] and of the scattering rate [9]. Alternatively, the short range CDW segments above 120 K might be considered as objects strongly scattering the free charge carriers. Within this

scenario the low energy response (*i.e.* long wave-length limit) is characterized by a free charge carriers contribution, while at higher frequency (*i.e.*, short wave-length limit) a local bound-state like excitation is expected to occur. This latter feature may give rise to the MIR absorption observed in both compounds. Therefore, the transport properties are dominated by strong electron-electron scattering, and when the phase-space is reduced by the CDW long range ordering, the scattering is likely to become less effective. The reduction of scattering due to partial gapping of the Fermi surface, may account for depression of the resistivity of 2H-TaSe$_2$ by two orders of magnitude between 120 and 4 K [9,10].

The CDW phase transition has much smaller effect on the electronic properties of 2H-NbSe$_2$. An inspection of the optical conductivity of 2H-NbSe$_2$ within the *ab*-plane does not reveal any peculiar feature below 5000 cm^{-1}, besides the effective metallic component (*i.e.*, zero energy mode) [11]. A clear gap signature is missing within the *ab*-plane (Fig. 1b) so that a comparison with other prototype CDW systems is difficult and less conclusive. Also, because spectroscopic hallmarks of the gap are not present in the data it is difficult to judge whether the narrowing of the metallic component is indicative of less effective scattering at $T < T_{CDW}$ or whether this effect merely reflects conventional drop of scattering due to electron-electron and/or electron-phonon processes. We also remark that in the measured spectral range for both compounds we did not find any evidence for collective excitations at $T < T_{CDW}$. Those excitations (if present) are expected to be active only in the microwave range, beyond the lower frequency limit of our measurements. Moreover, we also expect that such a collective excitation will be screened by the metallic component of the excitation spectrum. The absence of the collective excitation is also confirmed by the rather good agreement between $\sigma_1(\omega \to 0)$ and σ_{dc} (Fig. 1).

The CDW gap issue has been extensively debated in the literature. An ample discussion of this issue from the point of view of the optical experiments was already presented in references [9] and [23]. The possible evidence for the Peierls gap due to the formation of the CDW condensate has been addressed using other experimental probes, but conflicting results have been reported. Here, we would like to briefly recall a few representative work, emphasizing also those contributions not discussed in our previous publications [9–11]. We first quote two photoemission studies on 2H-TaSe$_2$ [24,25]. Both Dardel *et al.*'s [24] and Liu *et al.*'s [25] work, the latter one with the enhanced angle resolution, suggest that a small fraction of the Fermi surface is gapped by the CDW phase transitions, consistent with our observation of metallic optical response. Similar to optics and transport properties, these data are not affected by the incommensurate-commensurate CDW transition at 90 K. An estimation of the gap from the measured spectral function led to a gap value of about 160 meV [24]. Liu *et al.* [25] further pointed out that at $T > T_{CDW}$ two Fermi surfaces crossings occur along the $\Gamma - K$ direction and that a saddle band lies very close to

Fermi level E_F for an extended region along $\Gamma - K$. In the CDW state, the energy gap was found to be near zero at the first Fermi surface crossing and large in the saddle band region, in agreement with prediction from the "saddle-point" CDW mechanism by Rice and Scott [26].

Moreover, angle resolved photoemission (ARPES) data on 2H-NbSe$_2$ have shown that CDW in this compound is driven by Fermi surface nesting [27]. The same measurement showed the existence of saddle points near the Fermi surface, but their separation in k-space was found to be too large to account for the CDW periodicity observed in neutron scattering experiments [28]. ARPES data also suggested that CDW transition does not involve large modifications of the Fermi surface, in full agreement with our transport and optical results. On the other hand, more recent low temperature ARPES measurements on 2H-NbSe$_2$ revealed Fermi surface sheet-dependent superconductivity but no sign of CDW gap was detected [29]. Therefore, such a variety of conclusions based on photoemission data [24,25,27,29] does not resolve yet whether the CDW in these systems is driven by the saddle points or by the Fermi surface nesting. Probably, because of a significant warping of the Fermi surface in the *c*-direction, the nesting conditions might be satisfied only at certain k-points, not explored by ARPES. In this respect, Tonjes *et al.* suggest that the charge density waves in this family of materials originate from a combination of the partial nesting of the Fermi surface and the saddle band [30].

Finally, tunneling spectroscopy measurements have also revealed evidence for energy gaps in the density of states of both compounds. In 2H-TaSe$_2$ tunneling conductance spectra were suppressed below about 80 meV, associated with the CDW transition [31]. Similarly, in 2H-NbSe$_2$ a gap value of about 34 meV has been inferred. In both spectra, however, the suppression below the gap edge was not complete, in agreement with a partial gap in the density of states. Relative reduction on tunneling signal at zero bias was much stronger in 2H-TaSe$_2$ than in 2H-NbSe$_2$, supporting the evidence that the CDW transition has greater effect in the former compound. An independent tunneling measurement [32] on 2H-NbSe$_2$ found similar value of the CDW gap $\Delta_{CDW} = 34$ meV and a superconducting gap of about $\Delta_{SC} = 1.1$ meV, below T_c.

4.2 Quasiparticle coherence and interlayer response

As pointed out above, both 2H-TaSe$_2$ and 2H-NbSe$_2$ reveal metallic albeit strongly anisotropic response. In particular, the metallic form of the low temperature conductivity probed along the least conducting *c*-axis direction can be taken as evidence for band-like transport. However, the quantitative analysis of the conductivity data indicates that the interlayer response is not necessarily that trivial in particular in the 2H-TaSe$_2$ system. An estimate of the electronic mean free path (l) within a simple Drude model gives $l = 1$ Å for 2H-TaSe$_2$ along the *c*-direction (*i.e.*, much smaller than the lattice constant), while in the *ab*-plane $l = 16$ Å (*i.e.*, five times the lattice constant) [33]. A mean free path of the order of the lattice constant means that the out-of-plane dc transport is

beyond the Ioffe-Regel limit signaling a breakdown of the Boltzmann theory in connection to the c-axis response. An observation of a metal-like transport along the c-direction in the regime of extraordinary short mean free path is intriguing. Indeed, short mean free path implies the inadequacy of the ideas based on the concept of well defined quasiparticles and extended electronic states. In fact, the positive slope of $\rho_c(T)$ (*i.e.*, $\mathrm{d}\rho_c/\mathrm{d}T > 0$) [10] evokes the same puzzle for this conductor like for the whole class of materials with narrow bands, often referred to as *bad metals*. The latter group includes a diverse class of synthetic conductors such as cuprates, fullerenes, manganites and several different organic materials [34–36] which all show metal-like transport with positive $\mathrm{d}\rho_c/\mathrm{d}T > 0$ observed in the regime of very high values of resistivity. The above dichotomy of high resistivities and of the positive slopes in the $\rho(T)$ is yet to be resolved. An interesting idea allowing one to reconcile the two conflicting trends involves charge self-organization effects in low-dimensional conductors [37]. While charge segregation into conducting and insulating regions is fairly well-documented for oxides, so far evidence for such effects has not been reported for dichalcogenides.

Another interesting feature of the optical response of bad metals is related to the redistribution of the electronic spectral weight in the conductivity data. Small changes of temperature or in some cases of magnetic field appear to affect the conductivity spectra over an extraordinary broad frequency region [38–51]. In many cases changes of the spectral weight $N(\omega)$ extend beyond the upper cut-off of the experimentally accessible frequency interval leading to apparent violations of the conductivity sum rule. The global sum rule $\int_0^\infty \mathrm{d}\omega\,\sigma_1(\omega) = \frac{4\pi n e^2}{m_e}$ insists that the total area under the conductivity spectra must remain constant since it is determined only by the density of electrons n and the mass of free electron m_e. In practice, integration is carried out only over limited albeit broad frequency range, and N (Eq. (1)) obtained by integrating the data even over a frequency region as broad as 1 eV appears to be temperature- or field-dependent. One notorious example of "sum rule violation" is the interlayer response of HTC superconductors [41–43,52–54]. The effect is particularly strong in the so-called underdoped materials in which T_c is suppressed due to a reduction of carrier density from the "optimal" value delivering the maximum T_c for a given series. In these systems the superconducting transition is preceded by the formation of the pseudogap state at $T^* > T_c$. Development of the pseudogap state is associated with loss of the spectral weight in the c-axis conductivity. In the superconducting state excessive spectral weight emerges under the superconducting δ-function at $\omega = 0$. Ioffe and Millis [55] suggested that such a peculiar behaviour of the sum rule is a natural consequence of the superconducting pairing without long-range phase coherence, which leads to a factor of two (*i.e.*, 50%) of the missing spectral weight [55]. Within this scenario the apparent violation of the c-axis sum rule is not expected for short-range spin or charge density wave order. The full recovery of spectral weight within the MIR spectral range

in both dichalcogenide compounds and for both polarization directions (Fig. 2) is a convincing demonstration of the different nature of the relevant correlations involved in the CDW ground state. This result argues against the direct connection of the pseudogap state in HTC cuprates to the charge-density-wave order/fluctuations.

Further insights into unconventional features of the quasiparticle response of the studied dichalcogenides is provided by the scattering rate analysis of the data. As pointed out in reference [9], the width of the zero-energy mode in $\sigma_1(\omega)$ in the ab-plane response as well as the $\rho_{ab}(T)$ for 2H-TaSe$_2$ both display a noticeable decrease below $T_{1\mathrm{CDW}}$. This result can be naturally attributed to a depletion of the scattering channels associated with q-vectors of the Fermi surface's pockets involved in the CDW condensate [56]. This effect is weaker in 2H-NbSe$_2$ possibly due to the fact that the phase space affected by the CDW state is smaller. Another interesting distinction between 2H-NbSe$_2$ and 2H-TaSe$_2$ is related to the absolute values of the in-plane scattering rate. Interestingly, the scattering rate in 2H-TaSe$_2$ (Fig. 4) is always greater than the quasiparticle energy $1/\tau_{ab}(\omega) > \omega$. On the other hand, $1/\tau_{ab}(\omega)$ for 2H-NbSe$_2$ at 10 K is in a so-called Landau-Fermi liquid region where the quasiparticles are well defined, *i.e.* their energy is always larger than their scattering rate: $1/\tau_{ab}(\omega) < \omega$ (Ref. [52]). Small absolute values of $1/\tau_{ab}(\omega)$ also imply that the life-time of the well-defined quasiparticles is sufficiently long so that they can propagate coherently many interatomic distances both along and across the layers. Estimates based on both 3D and 2D free electron gas give the in-plane mean free path of ~ 100 Å and the out-of-plane of ~ 20 Å (Ref. [11]). The latter result is in full accord with de Haas-van Alphen measurements [4] that found a 3D Fermi surface in 2H-NbSe$_2$ at low temperatures. Remarkably, the depression of the interlayer conductivity in 2H-TaSe$_2$ compared to that of 2H-NbSe$_2$ correlates with stronger inelastic scattering probed within the ab-plane of the former compound (Fig. 4). Similar trend is also followed in a variety of HTC superconductors, as pointed out in reference [11], suggesting suppression of the interlayer tunneling in a system of poorly defined quasiparticles.

Finally, we note that the spectra of $1/\tau_{ab}(\omega)$ in both dichalcogenides are characterized by nearly linear frequency dependence at $\omega > 500$ cm^{-1}. A similar linear component in the in-plane scattering rate has also been found in other 2D conductors, graphite [57] and a number of cuprates [15]. The linear scattering rate deviates from the electron-electron Fermi liquid form $1/\tau_{ab}(\omega) \sim \omega^2$ observed in simple 3D metals, such as cerium [58], molybdenum [59] and chromium [18,60]. However some theoretical calculations [61,62] indicate that a quasi-2D electron gas is expected to show $1/\tau(\omega) \sim \omega$ dependence.

5 Conclusion

We have presented a detailed infrared spectroscopy study of the anisotropic dichalcogenide systems 2H-TaSe$_2$ and 2H-NbSe$_2$. The spectra of both compounds are metallic-like for both directions (*i.e.*, within the ab-plane and along

the c-axis), with the anisotropy effects being more pronounced in 2H-TaSe$_2$. The in-plane optical conductivity displays features that bear similarities with other classes of 2D materials, including HTC systems. We failed to detect spectral features directly attributable to the CDW gap in both compounds. This may be related to the fact that the charge density modulation affects only a small fraction of the Fermi surface. The influence of the CDW state is better resolved through the analysis of the carrier dynamics. We find that the experimental displays of the pseudogap state in carrier dynamics of cuprates HTS are much more prominent than the features attributable to the CDW response in the dichalcogenides. These results argue against the decisive role of incommensurate density waves in the formation of the pseudogap state in cuprates. The quantitative analysis of the conductivity data suggests that the transport properties of 2H-TaSe$_2$ (unlike the 2H-NbSe$_2$ counterpart) are in the regime pushing the boundaries of applicability of the Boltzmann theory. Indeed, in this system the in-plane scattering rate exceeds the energy, indicative of poorly defined quasiparticles, whereas the mean free path along the c-axis direction is shorter than the lattice spacings. Commonly, the above characteristics are taken as generic attributes of bad metal behavior. Nevertheless, the spectral weight distribution with apparent violation of the oscillator strength sum rule are not found in either of the investigated dichalcogenides, in contrast to the behavior of many other classes of bad metals.

References

1. E. Abrahams, S.V. Kravchenko, M.P. Sarachik, Rev. Mod. Phys. **73**, 251 (2001)
2. M.A. Kastner, R.J. Birgeneau, G. Shirane, Y. Endoh, Rev. Mod. Phys. **70**, 897 (1998)
3. J.A. Wilson, F.J. Di Salvo, S. Machajan, Adv. Phys. **24**, 117 (1975)
4. R. Corcoran, P. Meeson, Y. Onuki, P.-A. Probst, M. Springford, K. Takita, H. Harima, G.Y. Guo, B.L. Gyorffy, J. Phys. Cond. Matt. **6**, 4479 (1994)
5. H.J. Schulz, in *Strongly Correlated Electronic Materials*, edited by K.S. Bedell (Addison Wesley, Reading MA, 1994)
6. D.B. Tanner, T. Timusk, in *Physical Properties of high Temperature Superconductors III*, edited by D.M. Ginsberg (World Scientific, Singapore, 1992), p. 363 and references therein
7. L. Degiorgi, Rev. Mod. Phys. **71**, 687 (1999)
8. D.N. Basov, T. Timusk, in *Infrared Properties of High-T$_c$ Superconductors: An Experimental Overview, Handbook on the Physics and Chemistry of Rare Earths,* Vol. 31 (Elsevier Science BV, 2001), p. 437
9. V. Vescoli, L. Degiorgi, H. Berger, L. Forró, Phys. Rev. Lett. **81**, 453 (1998)
10. B. Ruzicka, L. Degiorgi, H. Berger, R. Gaál, L. Forró, Phys. Rev. Lett. **86**, 4136 (2001)
11. S.V. Dordevic, D.N. Basov, R.C. Dynes, E. Bucher, Phys. Rev. B **64**, 161103(R) (2001)
12. C.S. Oglesby, E. Bucher, C. Kloc, H. Hohl, J. Cryst. Growth **137**, 289 (1994)
13. J. Edwards, R.F. Frindt, J. Phys. Chem. Solids **32**, 2217 (1971)
14. F. Wooten, in *Optical Properties of Solids* (Academic Press, New York, 1972)
15. A.V. Puchkov, D.N. Basov, T. Timusk, J. Phys. Cond. Matt. **8**, 10049 (1996)
16. K. Kornelsen, J.E. Eldridge, C.C. Homes, H.H. Wang, J.M. Williams, Solid State Commun. **72**, 475 (1989)
17. P. Haas, E. Griesshaber, B. Gorshunov, D. Schweitzer, M. Dressel, T. Klausa, W. Strunz, F.F. Assaad, Phys. Rev. B **62**, R14673 (2000)
18. D.N. Basov, E.J. Singley, S.V. Dordevic, Phys. Rev. B **65**, 054516 (2002)
19. G. Gruner, in *Density Waves in Solids* (Addison-Wesley, Reading MA, 1994)
20. B.P. Gorshunov, A.A. Volkov, G.V. Kozlov, L. Degiorgi, A. Blank, T. Csiba, M. Dressel, Y. Kim, A. Schwartz, G. Gruner, Phys. Rev. Lett. **73**, 308 (1994)
21. L. Degiorgi, B. Alavi, G. Mihaly, G. Gruner, Phys. Rev. B **44**, 7808 (1991)
22. M. Dressel, A. Schwartz, G. Gruner, L. Degiorgi, Phys. Rev. Lett. **77**, 398 (1996)
23. A.S. Barker Jr., J.A. Ditzenberger, F.J. Di Salvo, Phys. Rev. B **12**, 2049 (1975)
24. B. Dardel, M. Grioni, D. Malterre, P. Weibel, Y. Baer, F. Levy, J. Phys. Cond. Matt. **5**, 6111 (1993)
25. R. Liu, C.G. Olson, W.C. Tonjes, R.F. Frindt, Phys. Rev. Lett. **80**, 5762 (1997)
26. T.M. Rice, G.K. Scott, Phys. Rev. Lett. **35**, 120 (1975)
27. Th. Straub, Th. Finteis, R. Claessen, P. Steiner, S. Hufner, P. Blaha, C.S. Oglesby, E. Bucher, Phys. Rev. Lett. **82**, 4504 (1999)
28. D.E. Moncton, J.D. Axe, F.J. DiSalvo, Phys. Rev. Lett. **35**, 734 (1975)
29. T. Yokoya, T. Kiss, A. Chainani, S. Shin, M. Nohara, H. Takagi, Science **294**, 2518 (2001)
30. W.C. Tonjes, V.A. Greanya, R. Liu, C.G. Olson, P. Molinié, Phys. Rev. B **63**, 235101 (2001)
31. C. Wang, B. Giambattista, C.G. Slough, R.V. Coleman, M.A. Subramanian, Phys. Rev. B **42**, 8890 (1990)
32. H.F. Hess, R.B. Robinson, R.C. Dynes, J.M. Valles, Jr., J.V. Waszczak, J. Vac. Sci. Technol A **8**, 450 (1990)
33. $l \sim (n^{-2/3})/\rho$, where ρ is the 300 K value of the resistivity [9,10] and the charge carrier concentration is from Hall effect measurement by D.A. Whitney, R.M. Fleming, R.V. Coleman, Phys. Rev. B **15**, 3405 (1977)
34. S.L. Cooper, K.E. Gray, in *Physical Properties of High Temperature Superconductors IV*, edited by D.M. Ginsberg (Singapore, World Scientific, 1994), p. 61
35. N.E. Hussey, M. Kibune, H. Nakagawa, N. Miura, Y. Iye, H. Takagi, S. Adachi, K. Tanabe, Phys. Rev. Lett. **80**, 2909 (1998)

36. V.J. Emery, S.A. Kivelson, Phys. Rev. Lett. **74**, 3253 (1995)
37. Y. Ando, A.N. Lavrov, S. Komiya, K. Segawa, X.F. Sun, Phys. Rev. Lett. **87**, 017001 (2001)
38. M.J. Rozenberg, G. Kotliar, H. Kajueter, G.A. Thomas, D.H. Rapkine, J.M. Honig, P. Metcalf, Phys. Rev. Lett. **75**, 105 (1995)
39. M. Imada, A. Fujimori, Y. Tokura, Rev. Mod. Phys. **70**, 1039 (1998)
40. Z. Schlesinger, Z. Fisk, H.-T. Zhang, M.B. Maple, J. DiTusa, G. Aeppli, Phys. Rev. Lett. **71**, 1748 (1993)
41. C.C. Homes, T. Timusk, R. Liang, D.A. Bonn, W.N. Hardy, Phys. Rev. Lett. **71**, 1645 (1993)
42. D.N. Basov, T. Timusk, B. Dabrowski, J.D. Jorgensen, Phys. Rev. B **50**, 3511 (1994)
43. D.N. Basov, H.A. Mook, B. Dabrowski, T. Timusk, Phys. Rev. B **52**, R13141 (1995)
44. S. Tajima, J. Schützmann, S. Miyamoto, I. Terasaki, Y. Sato, R. Hauff, Phys. Rev. B **55**, 6051 (1997)
45. C. Bernhard, D. Munzar, A. Wittlin, W. König, A. Golnik, C.T. Lin, M. Kläser, Th. Wolf, G. Müller-Vogt, M. Cardona, Phys. Rev. B **59**, R6631 (1999)
46. M. Rubhausen, A. Gozar, M.V. Klein, P. Guptasarma, D.G. Hinks, Phys. Rev. B **63**, 224514 (2001)
47. H.L. Liu, S.L. Cooper, S.-W. Cheong, Phys. Rev. Lett. **81**, 4684 (1998)
48. Y. Okimoto, T. Katsufuji, T. Ishikawa, A. Urushibara, T. Arima, Y. Tokura, Rev. Lett. **75**, 109 (1995)
49. S.G. Kaplan, M. Quijada, H.D. Drew, D.B. Tanner, G.C. Xiong, R. Ramesh, C. Kwon, T. Venkatesan, Phys. Rev. Lett. **77**, 2081 (1996)
50. K.H. Kim, J.H. Jung, D.J. Eom, T.W. Noh, J. Yu, E.J. Choi, Phys. Rev. Lett. **81**, 4983 (1998)
51. S. Broderick, B. Ruzicka, L. Degiorgi, H.R. Ott, J.L. Sarrao, Z. Fisk, Phys. Rev. B **65**, 121102(R) (2002)
52. S.V. Dordevic, E.J. Singley, D.N. Basov, S. Komiya, Y. Ando, E. Bucher, C.C. Homes, M. Strongin, Phys. Rev. B **65**, 134511 (2002)
53. D.N. Basov, S.I. Woods, A.S. Katz, E.J. Singley, R.C. Dynes, M. Xu, D.G. Hinks, C.C. Homes, M. Strongin, Science **283**, 49 (1999) and references therein
54. P.W. Anderson, Science **268**, 1184 (1995)
55. L.B. Ioffe, A.J. Millis, Science **285**, 1241 (1999)
56. T. Valla, A.V. Fedorov, P.D. Johnson, J. Xue, K.E. Smith, F.J. DiSalvo, Phys. Rev. Lett. **85**, 4759 (2000)
57. S. Xu, J. Cao, C.C. Miller, D.A. Mantell, R.J.D. Miller, Y. Gao, Phys. Rev. Lett. **76**, 483 (1996)
58. J.W. van der Eb, A.B. Kuz'menko, D. van der Marel, Phys. Rev. Lett. **86**, 3407 (2001)
59. T. Valla, A.V. Fedorov, P.D. Johnson, S.L. Hulbert, Phys. Rev. Lett. **83**, 2085 (1999)
60. The experimental data for simple metals like Cu, Au or Ag are not available
61. J. Gonzalez, F. Guinea, M.A.H. Vozmediano, Phys. Rev. Lett. **77**, 3589 (1996)
62. P.W. Anderson, Phys. Rev. B **55**, 11785 (1997)